Lab on a Chip

Sample-to-Analysis Platform for Rapid Intracellular Mass Spectrometry from Small Numbers of Cells

Journal:	*Lab on a Chip*
Manuscript ID	LC-ART-09-2021-000884.R1
Article Type:	Paper
Date Submitted by the Author:	25-Oct-2021
Complete List of Authors:	Culberson, Austin; Georgia Institute of Technology, The George W. Woodruff School of Mechanical Engineering Chilmonczyk, Mason; Georgia Institute of Technology, The George W. Woodruff School of Mechanical Engineering Kottke, Peter; Georgia Institute of Technology, The George W. Woodruff School of Mechanical Engineering Bowles-Welch, Annie; Georgia Institute of Technology, Marcus Center for Therapeutic Cell Characterization and Manufacturing, Parker H. Petit Institute for Bioengineering and Bioscience Ghoshal, Delta; Georgia Institute of Technology, The Wallace H. Coulter Department of Biomedical Engineering Fedorov, Andrei; Georgia Institute of Technology, The George W. Woodruff School of Mechanical Engineering

ARTICLE

Sample-to-Analysis Platform for Rapid Intracellular Mass Spectrometry from Small Numbers of Cells

Received 00th January 20xx,
Accepted 00th January 20xx

DOI: 10.1039/x0xx00000x

Austin L. Culberson,[a] Mason A. Chilmonczyk [a], Peter A. Kottke [a], Annie C. Bowles-Welch[b], Delta Ghoshal[c], and Andrei G. Fedorov[a] *

Real-time, advanced diagnostics of the biochemical state within cells remains a significant challenge for research and development, production, and application of cell-based therapies. The fundamental biochemical processes and mechanisms of action of such advanced therapies are still largely unknown, including the critical quality attributes that correlate to therapeutic function, performance, and potency and the critical process parameters that impact quality throughout cell therapy manufacturing. An integrated microfluidic platform has been developed for in-line analysis of a small number of cells via direct infusion nano-electrospray ionization mass spectrometry. Central to this platform is a microfabricated cell processing device that prepares cells from limited sample volumes removed directly from cell culture systems. The sample-to-analysis workflow overcomes the labor intensive, time-consuming, and destructive nature of existing mass spectrometry approaches for analysis of cells. By providing rapid, high-throughput analyses of the intracellular state, this platform enables untargeted discovery of critical quality attributes and their real-time, in-process monitoring.

Introduction

Utilizing cells for therapeutic applications is revolutionizing medicine by providing cures for previously incurable diseases[1, 2] and treatment of previously irreparable injuries.[3] These treatments, which rely on cells as either a drug production mechanism (e.g., monoclonal antibodies secreted from cells) or are directly used as the therapy (e.g., cell therapies), present unique development and biomanufacturing challenges compared to traditional small molecule pharmaceuticals. Rather than controlling the synthesis of a limited number of chemicals, cell-based therapies require not only characterization of the cell state, but also control of the complex and dynamic cell culture system as a whole.[4, 5] This presents a challenge for in-process control as existing real-time monitoring capabilities for biomanufacturing have been traditionally confined to indirect measures of culture viability such as temperature, pH, and dissolved gas.[6] Direct monitoring of biochemicals in the extracellular environment (e.g., cell media) via various spectroscopic methods has vastly improved insight into bioprocess systems. These methods, however, are largely constrained to monitoring a limited number of the highest abundance species (e.g., lactose and glutamine) in culture media.[7, 8] As such, they provide little information as to the actual state of manufactured cells, effectively measuring time delayed and spatially averaged effects of cell metabolism.

Direct analysis of the intracellular content provides valuable insight into the cellular state including differentiation stage, metabolic state, and overall health.[9] In the context of biomanufacturing, knowledge of the cell state can provide critical insight into the safety, efficacy, and potency of the final cell therapy product. Greater understanding of the intracellular biochemical environment can be leveraged to reduce developmental timelines in research settings by identifying CQAs and generating associated models at the systems biology level.[10] These models can in turn be used to optimize production processes by identifying, tracking, and controlling critical process parameters (CPPs) and their resulting impact on critical quality attributes (CQAs) of cell therapies.[11]

[a] *The George W. Woodruff School of Mechanical Engineering, Georgia Institute of Technology, Atlanta, GA, United States.*
[b] *Marcus Center for Therapeutic Cell Characterization and Manufacturing, Parker H. Petit Institute for Bioengineering and Bioscience, Georgia Institute of Technology, Atlanta, GA, United States.*
[c] *The Wallace H. Coulter Department of Biomedical Engineering, Georgia Institute of Technology and Emory University, Atlanta, GA, United States.*
** Corresponding Author: AGF@gatech.edu*

Existing intracellular analysis capabilities are largely constrained to downstream, targeted assays capable of detecting a limited number (and often only the most abundant) biochemicals. With over 23,000 unique biochemicals identified so far in the human metabolome, these methods are inadequate to fully characterize the cell state at a single time point, much less provide sufficient information for system level biology or in-process monitoring and control.[12] As such, significant interest has been shown in the development and deployment of existing offline analytical technologies for intracellular characterization to increase the breadth and depth of biochemical coverage. Given the sensitivity and specificity of mass spectrometry (MS) over a broad range of biochemical molecular weight, class, and concentration, MS is well positioned to provide detailed analysis of the intracellular state.[9, 13] Specifically, electrospray ionization mass spectrometry (ESI-MS) takes advantage of liquid phase ionization amenable for direct infusion analysis of complex mixtures. At this time, however, sample preparation requirements limit the capabilities of ESI-MS to offline applications and preclude its use for in-process monitoring.

Ideally, an MS-based workflow would provide broad biochemical coverage with minimal sample preparation from minimal sample sizes. Conventional intracellular mass spectrometry workflows, however, require tedious, manual, and time-consuming sample preparation.[14, 15] The limited throughput of such workflows restricts the data available for system level biology and CPP/CQA identification needed for the development of new cell-based therapies.[16] With lengthy processing times, these workflows are also unable to capture the dynamic and heterogeneous nature of *in vitro* cell growth, especially internal metabolic processes with times scales on the order of minutes.[17] The various preparatory steps (e.g., rinse, spin down, extraction, and concentration) are also performed in a batch manner and are not suitable for integration in a partially or fully automated production environment. In contrast, ambient ionization mass spectrometry approaches have demonstrated highly sensitive and specific biochemical detection directly from samples with minimal sample preparation.[18-22] However, the initial extraction step of these techniques (whether solvent based or spatially resolved ionization) is a pre-treatment that targets only specific classes of biochemicals based on solubility or location in the sample. These techniques are also largely limited to applications with spatial access to immobilized cells or whole tissue samples and are not conducive to in-process monitoring of cell production systems such as stirred tank bioreactors.

Even if sample pre-treatment were optimized and reduced, the need for significant numbers of cells (ranging from hundreds of thousands to millions)[14] to provide sufficient analytes for detection following sample preparation prohibits frequent, near continuous, in-process sampling directly from cell cultures. The need for such a large number of cells also prevents MS from being used as a quality control measure for donor qualification or product release of cell therapies given the irreplaceable value of each cell at both early and late time points of biomanufacturing. The sample volume needed for manual manipulation alone could result in significant perturbations of smaller production systems, especially for autologous cells, if frequent monitoring were desired. The pursuit of reduced sample size requirements has led to the emergence of single cell mass spectrometry. This field has generated important advances regarding processes internal to the cell by detection of both metabolites and proteins from individual cells. The rapidly growing body of literature on single cell MS highlights its capabilities for biomarker identification and biochemical pathway modelling in research settings.[23-26] These techniques, however, rely heavily on elaborate cell micro-manipulation to ensure only the intracellular environment is sampled, which limits the utility of these techniques for in-line continuous monitoring

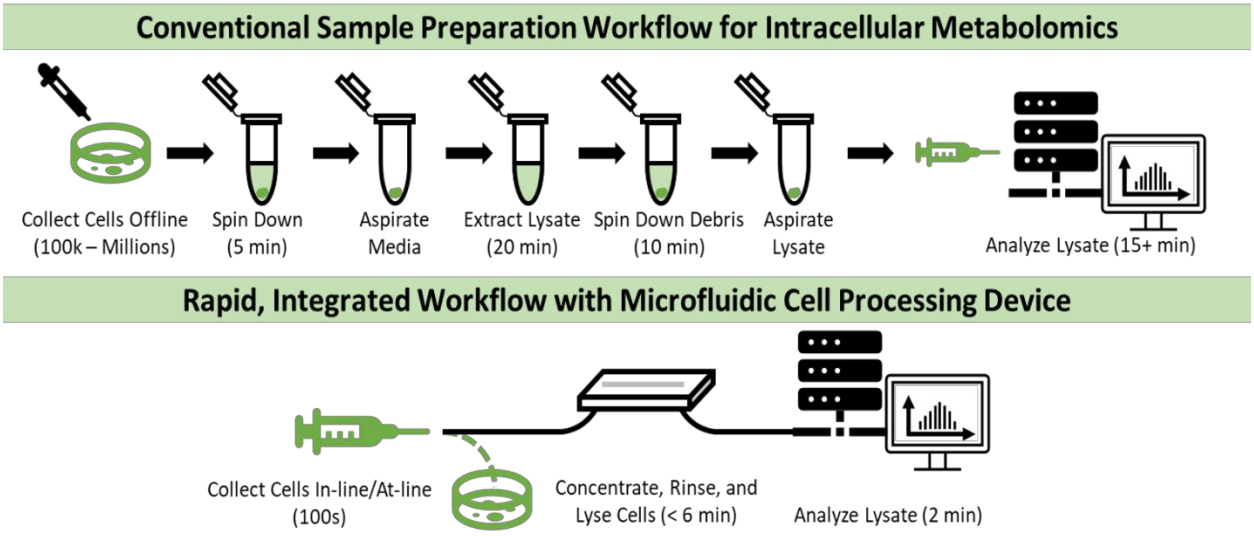

of the cell population state in a biomanufacturing workflow.

Figure 1. Conventional mass spectrometry intracellular metabolomics workflows (top) require time consuming sample preparation of large numbers of cells in manually prepared batches. The presented workflow (bottom) enables direct from culture sampling, automated sample preparation in a microfluidic device, and rapid ESI-MS. The sample-to-analysis integration removes manual handling, reduces analysis time, and enables analysis of small numbers of cells.

Though significant efforts have been made to increase throughput, minimize analysis times, reduce sample size, and eliminate manual handling through automation of the various aspects of conventional intracellular mass spectrometry (including in-line/at-line sample uptake, sample preparation, and sample introduction), fully integrated and rapid sample-to-analysis MS workflows have remained elusive.[13, 27-29] The mismatch between the highly variable, complex, and dynamic cell systems that need to be analyzed and the monitoring capabilities of mass spectrometry must be overcome to enable rapid intracellular analysis directly from culture. In this work, we present a new sample-to-analysis platform to effectively bridge the gap between cell system evolution and real-time MS analysis by taking small samples of cells directly from culture and performing a minimum number of processing steps for near continuous monitoring as shown in Figure 1. Rather than focusing on the comprehensive analysis (as is the goal of conventional workflows) or cell-by-cell targeted investigation (as is the goal of single cell workflows), this new process analytical technology enables dynamic characterization of the cell state directly from the growth environment with untargeted detection of a sufficiently broad range of relevant biomarkers, including intracellular metabolites.

Central to the platform is a microfluidic cell processing device capable of preparing ultra-small cell samples (on the order of hundreds of cells compared to hundreds of thousands needed for conventional workflows) for direct infusion ESI-MS. The device incorporates the critical aspects of conventional MS intracellular workflows (e.g., isolation, rinsing, and extraction) in a flow through format for rapid (less than 10 minute) analysis with no manual handling following sample uptake. The microfluidic design allows for minimum dilution of the sample prior to analysis; this is critical for achieving high sensitivity while requiring minimal cell samples. The device is coupled to a microcapillary sampling probe for direct-from-culture cell uptake (upstream) and an in-line nanoESI emitter for direct infusion to MS (downstream). By reducing the delay from “sampling to spectra”, the platform significantly increases the temporal resolution of bioprocess monitoring. The system is also designed such that it can be regenerated following each analysis cycle to provide near continuous monitoring in a single, integrated, and reusable format. These capabilities, alone or in combination with other approaches (e.g., secretome and transcriptome analyses), enable enhanced control of cell processes for both basic research applications as well as clinical production. The following study demonstrates the utility of this platform for intracellular characterization of cell therapies with focus on: 1) overview of the platform, including key design aspects; 2) demonstration of the utility of the workflow for detecting intracellular metabolites directly from culture; 3) system design and operating conditions, including microfabrication details, that enable dynamic monitoring using small numbers of cells.

Integrated Microfluidic Workflow

As shown in Figure 2, the integrated workflow starts with cell uptake via the sampling interface followed by sample conditioning in the cell processing device before direct, in-line ESI-MS analysis. During sample uptake, a syringe pump withdraws the desired volume at flowrates on the order of 50 nL/s from a cell culture system (e.g., well plates, culture dishes or flasks, stirred flask bioreactors) into the sample capillary. Extracting several hundred cells allows for sub-microliter volumes to be removed from the culture in a matter of seconds given typical cell culture concentrations. Removal of such small sample volumes has negligible impact on the total cell count or viability of the cell culture system, a critical requirement for frequent, in-process monitoring.

Following uptake, the cells are infused into the microfabricated cell processing device (Figure 2b). Within the device, cells are immobilized and concentrated in the cell lysis region using cell capture features (Figure 2c). Following capture, the concentrated cells are rinsed by continuously flowing 150 mM ammonium acetate. This rinse step removes the constituents of the cell culture media to ensure the analysis is solely representative of the intracellular content of cells, as well as eliminating ESI-MS interferants (e.g., salts) present at high concentrations in the cell media. Assuming complete dissolution, a 150 mM ammonium acetate solution translates to a 300 mOsm solution, approximating typical physiological osmolarity. Use of an iso-osmotic solution prevents uncontrolled osmotic lysis during rinsing which would result in time dependent release of the intracellular contents and subsequent dilution.[30] Furthermore, as a volatile additive, ammonium acetate reduces ion suppression during ESI-MS analysis compared to non-volatile salts present in the media and used in other isotonic buffers (e.g., PlasmaLyte).[31]

During rinsing, the flow downstream of the cell processing device is diverted to waste to prevent carryover effects and reduce clogging in the ESI emitter. Upon completion of a 3x volume rinse of the entire system, the flow is directed to the ESI emitter for direct infusion to the MS (approximately 4 minutes post sample collection). The intracellular contents are extracted via electrical pulses applied across the lysis electrodes (Figure 2b), resulting in irreversible poration of the cell membrane approximately 6 minutes post sample collection. Electrical lysis provides near-instantaneous release of the cellular contents, regardless of cell type, and is chosen in favor of chemically induced lysis techniques that could interfere with the detection of intracellular biochemicals.[32-34] The lysis step is initiated only after a stable ESI flow is established to ensure consistency of ESI-MS analyses (4-6 minutes post sample collection). Upon completion of the analysis of an infused sample, the system is regenerated by flowing a reconditioning buffer in the reverse direction to purge the system of cell debris and residual species (Figure 2c). This returns the system to its

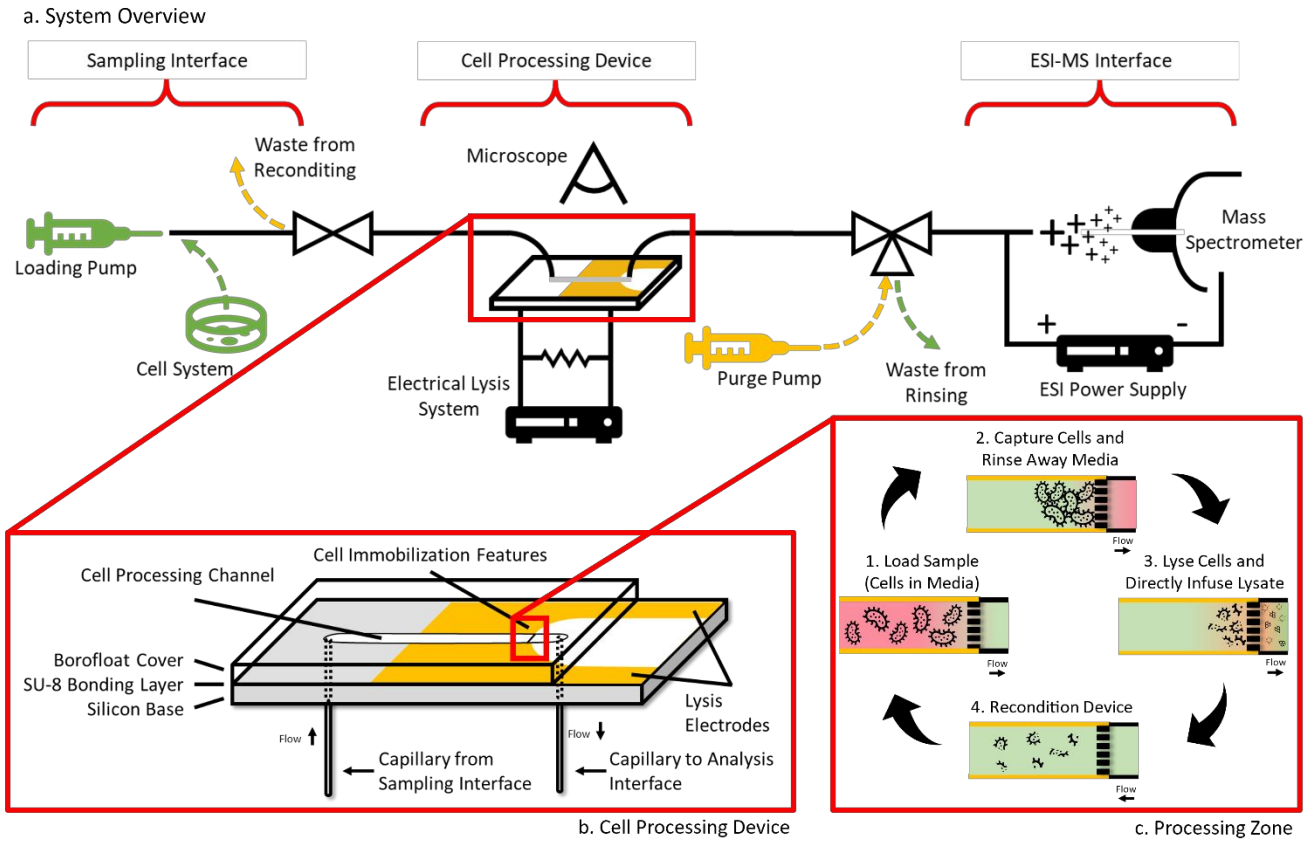

Figure 2. The integrated sample-to-analysis platform is composed of a sampling interface (left), cell processing device (middle), and ESI-MS interface (right). The analysis process begins with uptake of a cell laden sample directly from the cell system (e.g., petri dish, bioreactor, or vial). The sample plug is loaded into the microfabricated cell processing device (b). The silicon-based device is comprised of a microfluidic channel, cell immobilization features, and integrated electrodes. The device is sealed by a transparent, Borofloat cover bonded using an SU-8 adhesive layer. This allows the channel to be inspected via digital microscope throughout cell processing. In the device, cells are immobilized, rinsed, and lysed in the processing zone (c). During rinsing, the extracellular matrix is directed to waste; upon lysis, the downstream flow is diverted to the ESI interface for direct infusion ESI-MS. The system is then reconditioned by back flowing rinsing buffer via a secondary purge pump to remove cell debris from the microfluidic device prior to subsequent analyses.

initial state, ready for subsequent analyses such that a single device can be used repeatedly.

Detection of Metabolites from Cell Culture

The analytical workflow was applied to detect intracellular metabolites from a sample of approximately 1500 human umbilical vein endothelial cells (HUVECs). Figure 3 shows the resulting MS signal intensities for mass-to-charge values (m/z) corresponding to the protonated monoisotopic masses of the 20 amino acids found in the genetic code. As the building blocks of proteins and regulators of metabolism, amino acids represent an essential class of metabolites regardless of cell type.[35] Significant deviations from baseline physiological ranges (both excess and deficient) of particular acids can serve as disease markers for illnesses ranging from metabolic disorders[36] to neurodegenerative diseases.[37] Many amino acids have also been identified as CQAs for the development and characterization of new cell therapies, being up or down regulated in response to culture conditions[38] and serving as critical targets in disease modelling studies.[39] Amino acids also represent a diverse subset of metabolites ranging from hydrophobic to hydrophilic, having both charged and neutral species, and being present across several orders of magnitude of concentration within the cell, thus representing a comprehensive and clinically relevant testbed.

The top trace of Figure 3 represents the total ion current (TIC) for each MS scan; it displays minimal variation in the time period immediately following lysis, indicating stable ESI. Below the TIC, the amino acid traces are shown. The nearly constant TIC allows for interpretation of increases of signal intensity at specific m/z values to indicate the presence of a given amino acid in the cell lysate. Fourteen out of nineteen of the protonated monoisotopic mass traces displayed distinct signal intensity increases (as isomers, leucine and isoleucine cannot be distinguished without additional separation/analysis schemes and are thus represented by a single trace). The increases align with the anticipated elution characteristics (time delay and duration of the peak) and thus provide strong evidence of successful detection. Five amino acids (phenylalanine, tryptophan, methionine, cysteine, and arginine) showed either no or inconclusive increases in signal intensity. Given the mechanisms of ESI-MS, it is possible an analyte is present but not detectable at the protonated monoisotopic mass. In such cases, tracing possible adducts (i.e., amino acid plus Na^+, K^+, and

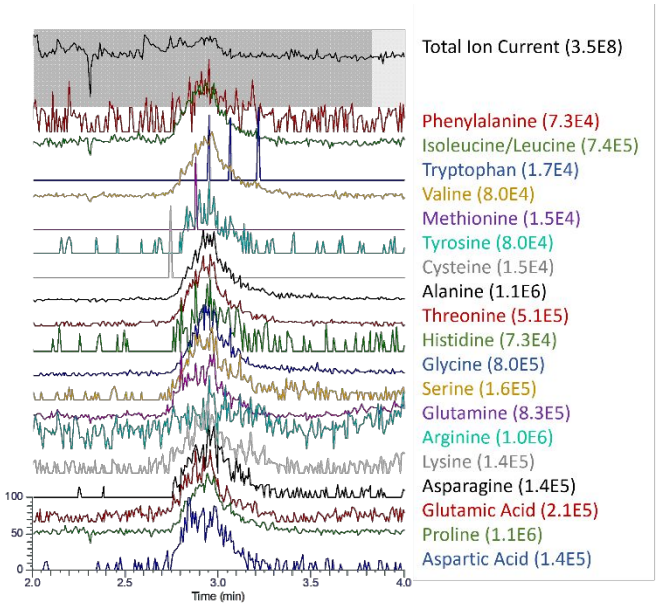

Figure 3. ESI-MS amino acid detection depicted as protonated monoisotopic m/z traces during the period immediately following lysis. The amino acids are sorted from most hydrophobic at top to most hydrophilic at bottom (at neutral pH). Recording of the MS signal begins following the rinsing step, approximately 4 minutes post sample uptake. The traces are shown immediately following lysis corresponding to 2 minutes post rinse or 6 minutes post sample uptake. The traces are normalized for each analyte with the maximum signal intensity given in parenthesis for the displayed time range.

NH_4^+) and potential fragmentation patterns provides additional means of detection. Open-source databases (MassBank of North America, MassBank Europe, and MZMine) were queried for common fragments identified using ESI-MS and compared against the sample spectra of the five undetected amino acids. Both methionine and arginine displayed distinct increases associated with the identified fragments (Supplementary Figure 3). While no fragments of phenylalanine were identified, the NH_4^+ adduct mass displayed a distinct signal increase (Supplementary Figure 4). This is consistent with the presence of NH_4^+ ions in solution following disassociation of ammonium acetate which is present in the rinsing buffer.

Even after tracking the protonated monoisotopic, fragment, and adduct masses, the absence of a distinct signal increase does not necessarily indicate the absence of an analyte. The ESI-MS analysis of multi-analyte solutions is dependent on a complex interplay of ionization potential, charge scavenging, and limit of detection for a given analyte. These complications are further exaggerated in complex solutions such as the cell lysate which is expected to contain thousands of electro-chemically distinct analytes distributed across several orders of magnitude in concentration. For example, cysteine and tryptophan are among the least abundant amino acids, and therefore likely fall below the limit of detection even though they are expected to be present within the cell.[40]

To further demonstrate the analytical capability of the sample-to-analysis platform, a more diverse segment of the metabolome clinically relevant specifically to HUVECs has been analyzed as shown in Figure 4. Jayaraman et al. identified intracellular metabolites significantly up or down-regulated when HUVECs were co-cultured with either highly metastatic or highly invasive prostate cancer cells.[39] These metabolites represent potential biomarkers and may provide targets for inhibiting cancer growth through metabolic control of endothelial cells in the tumor microenvironment. Figure 4 depicts the thirteen non-amino acid metabolite markers identified by Jayaraman et al. using positive mode ESI-MS with upstream high-performance liquid chromatography (HPLC); the five amino acids (L-glutamic acid, L-arginine, L-tryptophan, L-tyrosine, and methionine) identified in the study are included in the results of Figure 3. Of the protonated monoisotopic traces shown on the left of Figure 4 (sorted by descending m/z), only creatine showed a distinct elution band. Extending the analysis to include common fragments reported in open-source databases, seven additional analytes displayed distinct signal increases corresponding to the lysate elution band as seen on the right of Figure 4. In total, twelve of the eighteen metabolites (four amino acids and eight non-amino acid metabolites) identified by Jayaraman et al. were detected by our system. The remaining six undetected metabolites (hypoxanthine, guanine, cysteinylglycine, inosine, oleamide, and nicotinamide adenine dinucleotide) are likely missed due to charge scavenging, abundance below limit of detection, and/or ion suppression during ESI. Representative spectra of both detected and undetected metabolites are included in Supplementary Figure 5.

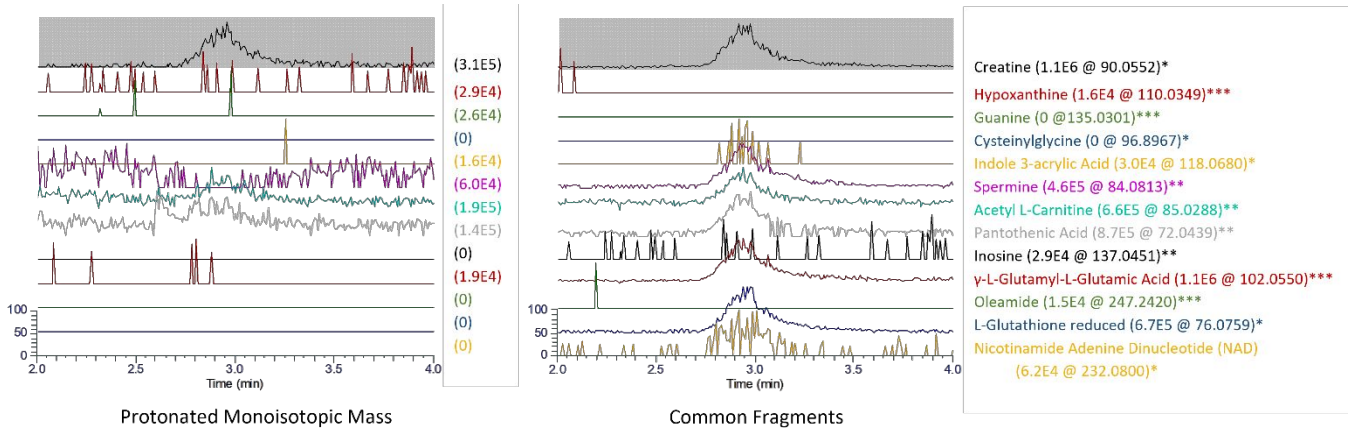

Figure 4. ESI-MS metabolite detection of relevance to HUVECs depicted as m/z traces during the period immediately following lysis. The metabolites are sorted by descending monoisotopic mass (left). The traces are normalized for each analyte by the maximum signal intensity (given in parenthesis) for the displayed time range. * Denotes fragments reported in MassBank of North America (MoNA), ** denotes fragments reported in MassBank Europe, ***denotes fragments reported in MZMine.

Effect of Sampled Number of Cells on Metabolite Detection

To characterize the sensitivity of the system to the number of cells up-taken, samples containing approximately 200, 500, and 1500 cells were analyzed. For the case of 200 cells, none of the traced analytes were detected in the anticipated lysate band. For the case of 500 cells, only three of the nineteen amino acids showed distinct signal increases at the protonated monoisotopic mass as shown in Supplementary Figure 6. For 1500 cells, 14 out of 19 amino acids were detected at the protonated monoisotopic mass as discussed in the previous sections.

The sensitivity to cell number is due both to system limitations and the broad dynamic range of intracellular metabolite concentrations. The number and concentration of intracellular molecules per cell varies for each species ranging from vanishingly small up to 10^{11} (mM range) molecules per cell.[23] The limit of detection also varies between analytes as determined by ionization potential and susceptibility to in-source modifications (i.e., adduct formation or fragmentation). Regarding system operation, the dilution factor following lysis is independent of cell number as the cells form a packed bed during the immobilization step. The dilution factor following dispersion is, however, dependent on the initial width of the lysate band, and thus the cell number. For the system described herein, the final dilution factor is approximately 0.4% for analysis of 100 cells. For a metabolite at an intracellular concentration of 1 µM, the average concentration in the dispersed lysate band at the emitter would be a mere 4 nM. Using a greater number of cells significantly reduces the final dilution, increasing the final concentration by nearly an order of magnitude for the case of 1000 cells (dispersion calculation details can be found in Supplementary Information). As such, the combination of both system and species dependent sensitivity yields non-uniform behavior in reaching the limit of detection across all analytes as a function of the number of cells used in the analysis.

Even with this unavoidable dependence on cell number, the developed sample-to-analysis platform detected seventeen out of nineteen amino acids and a majority (twelve out of eighteen) of HUVEC specific biomarkers from a very small sample of just 1500 cells. This is a significant analytical result, given that it was achieved using a small number of cells (vs hundreds of thousands or more) in a matter of minutes (versus hours) compared to conventional HPLC ESI-MS workflows. Collectively, these results demonstrate the capability for the developed microfluidic platform to operate in a quasi-continuous flow format for rapid assessment of the intracellular metabolome with broad biochemical coverage.

Fabrication, Characterization, and Operation

Microfabrication of Cell Processing Device

The cell processing device is manufactured using advanced microfabrication techniques, enabling integration of numerous features in a single device with opportunities for scaled production via batch processing. The details of the process are given in Supplementary Information with key elements of the design and processing sequence summarized here. Thirty-two devices, each with 10 mm x 15 mm footprint, are fabricated on a 4" diameter, 500 µm thick silicon wafer. The bulk of processing is centered around creation of microfluidic channels 5.075 mm long, 100 µm wide, and 30 µm deep. A series of parallel pillars spanning the channel width, each 5 µm wide with 3 µm spacing, serves as the cell immobilization feature (Figure 5). This design effectively

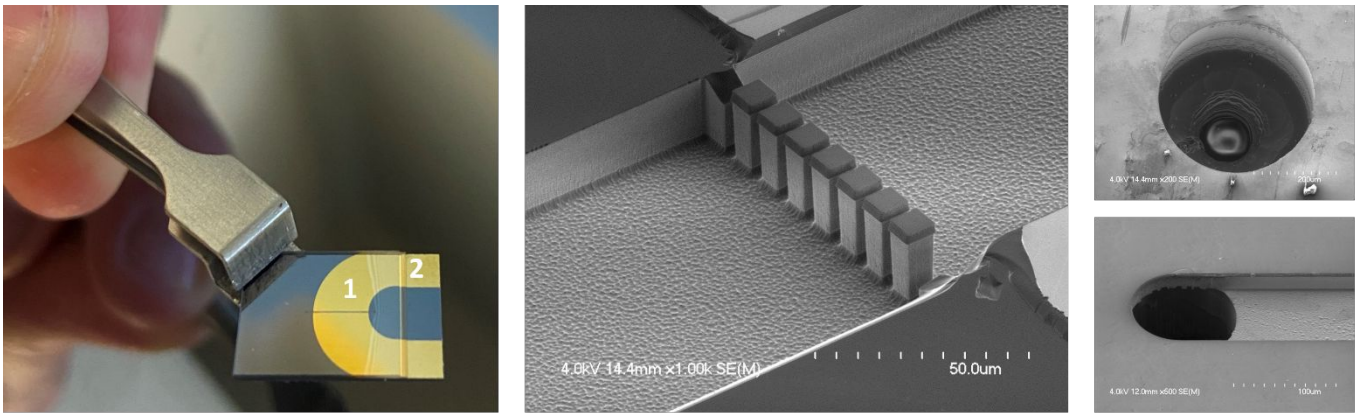

a. Cell Processing Device b. Cell Immobilization Features c. Inlet/Outlet Design

Figure 5. The cell processing device (a) is comprised of a microfluidic channel (a1) in a silicon base with integrated electrodes along the channel. The channel is sealed with a transparent Borofloat cover while allowing the ends of the electrodes to remain exposed to facilitate connecting to the lysis circuit (a2). A series of 5 µm wide pillars spans the microfluidic channel to prevent cells from passing further downstream and allow for rinsing prior to intracellular content extraction(b). Minimal dead volume inlet and outlet connections are made via the countersunk inlet design (not shown) to enable direct integration into the larger microfluidic workflow (c).

captures and concentrates the cells at the restriction point while allowing the media and rinsing buffer to continuously flow, thus avoiding clogging and high-pressure conditions that can lead to device delamination. Lysis electrodes are positioned along the channels and extend 3.975 mm upstream of the cell immobilization features. Gold was used as the electrode material as it will not corrode when exposed to the sample solution (the electrodes are in direct contact with fluid in the channel) and has favorable electromigration properties to withstand the repetitive application of high voltages applied across the thin layer. Inlet and outlet holes, 100 µm in ID, are etched through the silicon at the extents of the channel. Concentric to the through holes are 360 µm diameter counterbores which are etched approximately 250 µm deep. This design enables robust incorporation of 360 µm OD capillary inlet and outlet tubing for low dead volume fluidic connections.[41] The total device volume is 17 nL.

The channels are capped with a Borofloat 33 (Schott, Rye Brook, NY) cover. Borofloat is transparent and allows flow visualization within the device while having a coefficient of thermal expansion on the same order of magnitude as silicon to ensure thermomechanical compatibility during the bonding step. The Borofloat fully covers the fluidic channel while leaving a portion of the electrodes exposed at the edges of the device to serve as electrical pads for application of the lysis pulses. The Borofloat is bonded to the silicon wafer using an SU8-3005 adhesive layer (MicroChem, Westborough, MA). SU8 was chosen as it provides a water-insoluble, chemically inert bonding layer. Numerous studies have shown SU8 compatibility with MS, demonstrating it is resistant to common MS solvents, will not leach into the analysis fluid (resulting in polymer peaks), nor scavenge biochemicals from the sample by absorption[42] in contrast to other microfluidic device materials such as polydimethylsiloxane (PDMS).[43-45] Several devices were exposed to the electrical lysis pulse sequence with only buffer in the device to investigate the potential breakdown of SU8 in the presence of high electric fields. The resulting spectra showed no contaminants were released during the tests. This conclusion is in agreement with the electric breakdown field of SU8 which is reported as approximately 10^8 V/m, three orders of magnitude above the 6 kV/cm lysis pulse.[42]

The devices proved to be robust and reusable for multiple sequential measurements with no detectable carry-over between the runs. However, the risk of carryover in analysis of complex samples with such large ranges of biochemical concentrations is notable and could impact the reliability of the analytical output. Batch fabrication allows for dramatic reduction in the cost per device such that even single use becomes practical given the reduced burden of cell number, analytical effort, and analysis time. Following dicing of individual devices and attachment of inlet/outlet capillaries, the finished cell processing devices are held in a custom machined plexiglass fixture to facilitate orientation in front of the MS, ease connection of the lysis circuit to the electrodes, and allow real-time visualization of the channel via a digital microscope.

Fluidic System

With reference to Figure 2, the various fluidic components connecting the sampling and analysis interfaces to the cell processing device were designed to balance sample transit time, dead volume, pressure drop, and diffusion/dispersion effects. Detailed assessment of the trade-offs is given in Supplementary Information with the specific configuration detailed here. A LabSmith CapTite MV201-C360 3-port selector valve (LabSmith, Livermore, CA) with 130 nL swept volume connects the cell processing device to the flow conduit for sample regeneration and to the ESI emitter via 360 µm OD capillary. Other non-valved connections (e.g., between syringe and fluidic system) are via Valco ZU1XC zero volume unions (VICI Valco Instruments, Houston, TX). A 360 µm OD, 75 µm ID fused silica capillary is used upstream of the device to accommodate cell loading without clogging. The length of sampling capillary is such that the entire sampled volume is contained within; this allows for the syringe pump to be used in the withdraw/infuse manner without introducing cells into the syringe itself. Downstream of the device, 50 µm ID fused silica capillary is used to reduce transit time of the lysate volume while minimizing clogging and pressure drop. The length of capillary between the cell processing device and ESI emitter, as well as the emitter itself, are minimized to further reduce transit time, pressure drop, and dispersion effects.

Electrical Lysis Configuration and Operation

Lysis pulses are applied between the electrodes lining the cell processing channel as seen in Figure 5a. Prior to the lysis sequence, the leads of the lysis power supply are held at the same potential until a high voltage insulated gate bipolar transistor (IGBT) gate is closed according to the chosen pulse parameters (voltage, duration, and frequency) (Figure 6). Closing the gate completes the circuit internal to the lysis system, effectively draining the current across the high resistance network formed by the resistor and microfluidic channel. With electric leads on each side of the network, one electrode becomes the “source” and the other, the “drain”. This results in an electric potential difference between the electrodes sufficient for lysis. Once the gate is re-opened, there is no current flow and thus no voltage drop across the resistance network, allowing the “drain” to again float to an equal potential as the “source”. The lysis voltage is applied via a Stanford Research Systems PS350 High Voltage Power Supply (Stanford Research Systems, Sunnyvale, CA). The pulse duration, shape, and frequency are controlled by an Agilent 33250A waveform generator (Keysight Technologies, Santa Rosa, CA); a 5 Vpp, +2.5 V DC offset output signal is supplied to fully open and close the IGBT gate.

An IXYS IXYL60N450 IGBT (Littelfuse, Chicago, IL) enables high voltage, high power control with nanosecond switching times (MHz switching frequency). When not in operation, the entire lysis circuit is electrically isolated from the ESI electrical circuit by a switch to prevent uncontrolled electrolysis in the system, ensuring stability of the ESI-MS signal.

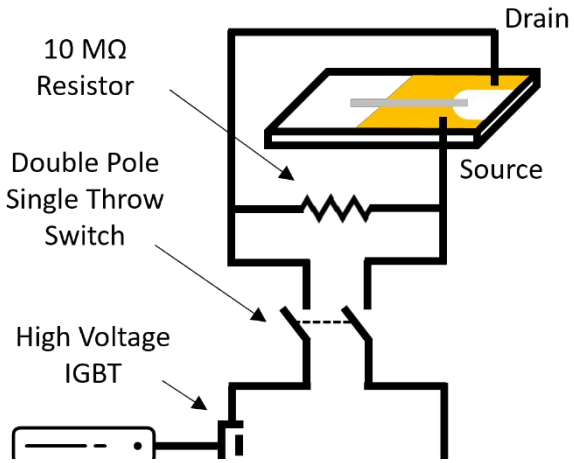

Figure 6. Electrical lysis circuit design. Leads are connected to each electrode lining the channel to provide potential difference sufficient for lysis according to the chosen pulse parameters. A high voltage IGBT enables rapid switching to open or close the circuit, allowing for one electrode to effectively drain or float based on the voltage drop across the resistance network. The switch allows for the system to be electrically isolated from the ESI circuit until lysis pulses are applied.

The lysis efficiency depends on an optimal combination of pulse amplitude, duration, and number for a given electrode configuration.[46] The applied voltage was set at 60 V, corresponding to an electric field across the 100 µm channel of 6 kV/cm. This value is within the electric field strength required for irreversible electroporation of mammalian cells (typically reported as >1 kV/cm or >1 V in terms of transmembrane potential).[46, 47] The pulse duration was then incrementally increased from microseconds to milliseconds and the extent of electrolysis in the channel was monitored. The pulse sequence of 1000, 5 ms square waves applied at 100 Hz was selected such that observable electrolysis occurred in the channel but did not result in bubbles that spanned the channel. Such limited electrolysis showed no appreciable impact on the ESI-MS signal but provides a visual cue that electrical lysis is performed. The combination of voltage and pulse sequence is in agreement with observations that longer duration pulses, even when applied at lower voltages, result in higher lysis efficiency compared to stronger but shorter duration pulses.[47] The efficiency further increases with a greater number of pulses, but must be balanced with the extent of electrolysis allowable to maintain ESI stability.

Conclusions

Mass spectrometry holds unparalleled potential for ultra-sensitive and specific intracellular biochemical analysis. At present, however, no MS based analytical technology is available that allows for continuous, temporally resolved monitoring of the intracellular metabolome. Further, conventional MS metabolomics is limited to working with relatively large samples containing extracts from hundreds of thousands of cells. This work presents a microfluidic platform and associated workflow to overcome these limitations. This integrated sample-to-analysis platform was applied to the intracellular analysis of 1500 HUVEC cells in native media sampled directly from a cell suspension system. The analysis enables detection of nearly all proteogenic amino acids as well as a majority of key metabolites identified as HUVEC specific biomarkers. Important to workflow validation, the developed platform has demonstrated the capability to detect clinically relevant intracellular biomarkers which have been previously identified using conventional HPLC ESI-MS. In addition to its demonstrated analytical power, the platform replaces the numerous manual handling steps with paths toward complete automation, works with ultra-small cell samples, is capable of self-regeneration for long-term, continuous operation, and is suitable for integration into cell growth bioreactors for direct-from-culture analysis. Continuous biochemical readout of the intracellular environment in real-time, as demonstrated in this work, is a critical milestone to enable fully automated quality monitoring with integrated feedback control in cell-based therapy manufacturing.

Experimental Methods

HUVEC Culture and Harvesting

Human umbilical vein endothelial cells (Lonza, Basel, Switzerland) were cultured in EGM-2MV (Lonza) on 150 cm^2 tissue culture flasks coated with 0.1% gelatin (Sigma-Aldrich, St. Louis, MO), in a 37 °C and 5% CO_2 incubator. Cells were harvested at passage 6 by rinsing with 1 mL/25cm^2 phosphate-buffered saline (Corning, Corning, NY), incubating with 1 mL/25cm^2 TrypLE (Thermo Fisher Scientific, Waltham, MA), and neutralizing with 1 mL/25cm^2 10% fetal bovine serum (Cytiva, Marlborough, MA) in PBS. Cells were then pelleted at 300 g for 5 minutes at 4 °C, resuspended in 1 mL/75cm^2 EGM-2MV, and counted using a Countess Automated Cell Counter (Thermo Fisher Scientific) using AOPI live cell discrimination (Nexcelom Bioscience, Lawrence, MA).

ESI-MS Analysis and Data Processing

Prior to analysis, the system was primed with the buffer flow to eliminate any bubbles that might disrupt ESI. Cells were sampled directly from a suspension in native media at an uptake flowrate of 150 µL/hr. The sample was loaded into the cell processing device and immediately rinsed by continuously flowing rinsing buffer for 4 minutes. The rinsing duration corresponds to a 3x rinse

of the entire system volume to ensure all media components are purged from the system. During the rinse, the downstream flow was diverted from the ESI emitter and directed to waste. Following the rinse, the flow was directed to the ESI emitter via the switching valve and the ESI voltage of ~4 kV was applied until stable ESI was established. Once stable ESI was observed (variation in total ion current less than 20%), the ESI voltage was turned off, the lysis circuit activated, lysis pulses applied approximately 2 min post rinse, and ESI immediately reinitiated for analysis. Protonation of analytes is promoted by addition of 0.1% acetic acid by volume to the buffer solution.

Data was acquired using a Thermo Scientific Q Exactive Plus Quadrupole-Orbitrap mass spectrometer (Thermo Fisher Scientific). The MS was operated in full scan positive mode with a mass range of 50–750 m/z and resolving power of 140,000 FWHM at 200 m/z. The automatic gain control (AGC) target was set to 1E6 with a maximum injection time of 500 ms; the S-Lens RF level was set to 40 to reduce fragmentation and ensure sensitivity at lower m/z values. Fused silica ESI emitters were fabricated in house from 360 μm OD, 100 μm ID capillary. The capillary was pulled to a fine point tip using a Sutter P-2000 Laser-Based Micropipette Puller System (Sutter Instrument, Novato, CA). The internal diameter of the emitter was enlarged by trimming the tip using an Optec Femtosecond laser (Optec Laser Systems, San Diego, CA); the laser allows for precise control of the final tip dimensions with a target ID of 15 μm to prevent clogging of the emitter while still enabling stable nanoESI. The emitter orientation in front of the MS and ESI voltage were adjusted until the AGC target was reached for each scan and variability in the total ion current was less than 20%. Data analysis was performed using Thermo Scientific FreeStyle software. Targeted analyses were performed using mass traces with 10 ppm mass tolerance for each anticipated m/z value. The protonated monoisotopic mass of each target analyte was initially queried with secondary traces according to m/z values of fragments reported in MassBank of North America (MoNA), MassBank Europe, or MZMine databases.

Author Contributions

A.G.F. and P.A.K. conceived of the idea for the microfluidic platform and formulated research goals. A.L.C. designed, built, validated, and applied the platform with assistance and supervision from M.A.C., P.A.K, and A.G.F. Cell culture, harvesting, and biological insight were provided by D.G. and A.C.B-W. A.L.C. interpreted results and wrote the initial draft with significant input from M.A.C., P.A.K, and A.G.F. The final draft was completed with assistance from all authors.

Conflicts of Interest

Mason Chilmonczyk and Andrei Fedorov are inventors of the technology and are pursuing its commercialization. The terms of this arrangement have been reviewed and approved by Georgia Tech in accordance with its conflict of interest policies.

Acknowledgements

The work described herein is supported by NSF Center for Cell Manufacturing Technologies (CMaT) Award 1648035, NSF Graduate Research Fellowship Grant No. DGE-1148903, the Marcus Center for Therapeutic Cell Characterization and Manufacturing Collaboration Grant in Cell Manufacturing, the Georgia Tech Foundation, and the Georgia Research Alliance. Partial support was also provided by Grant Number R01 GM138802 from the National Institute of General Medical Science (NIGMS), a component of the National Institutes of Health (NIH). Its contents are solely the responsibility of the authors and do not necessarily represent the official views of NSF, NIGMS or NIH. Device fabrication was performed at the Georgia Tech Institute for Electronics and Nanotechnology, a member of the National Nanotechnology Coordinated Infrastructure (NNCI), which is supported by National Science Foundation Grant ECCS-2025462. The authors would like to acknowledge the Roy lab, specifically Nate Dwarshuis and Miguel Armenta Ochoa, and the Marcus Center for Therapeutic Cell Characterization and Manufacturing (MC3M) staff for technical assistance with cell culture experiments.

References

1. Pittenger, M. F.; Discher, D. E.; Péault, B. M.; Phinney, D. G.; Hare, J. M.; Caplan, A. I., Mesenchymal stem cell perspective: cell biology to clinical progress. *npj Regenerative Medicine* **2019,** *4* (1), 22.
2. Sermer, D.; Brentjens, R., CAR T-cell therapy: Full speed ahead. *Hematological Oncology* **2019,** *37* (S1), 95-100.
3. Vismara, I.; Papa, S.; Rossi, F.; Forloni, G.; Veglianese, P., Current Options for Cell Therapy in Spinal Cord Injury. *Trends in Molecular Medicine* **2017,** *23* (9), 831-849.
4. Aijaz, A.; Li, M.; Smith, D.; Khong, D.; LeBlon, C.; Fenton, O. S.; Olabisi, R. M.; Libutti, S.; Tischfield, J.; Maus, M. V.; Deans, R.; Barcia, R. N.; Anderson, D. G.; Ritz, J.; Preti, R.; Parekkadan, B., Biomanufacturing for clinically advanced cell therapies. *Nature Biomedical Engineering* **2018,** *2* (6), 362-376.

5. Roh, K.-H.; Nerem, R. M.; Roy, K., Biomanufacturing of Therapeutic Cells: State of the Art, Current Challenges, and Future Perspectives. *Annual Review of Chemical and Biomolecular Engineering* **2016,** *7* (1), 455-478.
6. Biechele, P.; Busse, C.; Solle, D.; Scheper, T.; Reardon, K., Sensor systems for bioprocess monitoring. *Engineering in Life Sciences* **2015,** *15* (5), 469-488.
7. Abu-Absi, N. R.; Kenty, B. M.; Cuellar, M. E.; Borys, M. C.; Sakhamuri, S.; Strachan, D. J.; Hausladen, M. C.; Li, Z. J., Real time monitoring of multiple parameters in mammalian cell culture bioreactors using an in-line Raman spectroscopy probe. *Biotechnology and Bioengineering* **2011,** *108* (5), 1215-1221.
8. Landgrebe, D.; Haake, C.; Höpfner, T.; Beutel, S.; Hitzmann, B.; Scheper, T.; Rhiel, M.; Reardon, K. F., On-line infrared spectroscopy for bioprocess monitoring. *Applied Microbiology and Biotechnology* **2010,** *88* (1), 11-22.
9. Dettmer, K.; Aronov, P. A.; Hammock, B. D., Mass spectrometry-based metabolomics. *Mass spectrometry reviews* **2007,** *26* (1), 51-78.
10. May, M., Big data, big picture: Metabolomics meets systems biology. *Science Magazine* 2017, pp 646-648.
11. Consortium, N. C. M. *Achieving Large-Scale, Cost-Effective, Reproducible Manufacturing of High-Quality Cells: A Technology Road Map to 2025*; Office of Science, Technology, and Policy: 2016.
12. Wishart, D. S.; Feunang, Y. D.; Marcu, A.; Guo, A. C.; Liang, K.; Vázquez-Fresno, R.; Sajed, T.; Johnson, D.; Li, C.; Karu, N.; Sayeeda, Z.; Lo, E.; Assempour, N.; Berjanskii, M.; Singhal, S.; Arndt, D.; Liang, Y.; Badran, H.; Grant, J.; Serra-Cayuela, A.; Liu, Y.; Mandal, R.; Neveu, V.; Pon, A.; Knox, C.; Wilson, M.; Manach, C.; Scalbert, A., HMDB 4.0: the human metabolome database for 2018. *Nucleic Acids Res* **2018,** *46* (D1), D608-D617.
13. Lombard-Banek, C.; Schiel, J. E., Mass Spectrometry Advances and Perspectives for the Characterization of Emerging Adoptive Cell Therapies. *Molecules* **2020,** *25* (6), 1396.
14. Yuan, M.; Breitkopf, S. B.; Yang, X.; Asara, J. M., A positive/negative ion-switching, targeted mass spectrometry-based metabolomics platform for bodily fluids, cells, and fresh and fixed tissue. *Nat Protoc* **2012,** *7* (5), 872-81.
15. Courant, F.; Antignac, J.-P.; Dervilly-Pinel, G.; Le Bizec, B., Basics of mass spectrometry based metabolomics. *Proteomics* **2014,** *14* (21-22), 2369-2388.
16. Majumder, E. L. W.; Billings, E. M.; Benton, H. P.; Martin, R. L.; Palermo, A.; Guijas, C.; Rinschen, M. M.; Domingo-Almenara, X.; Montenegro-Burke, J. R.; Tagtow, B. A.; Plumb, R. S.; Siuzdak, G., Cognitive analysis of metabolomics data for systems biology. *Nature Protocols* **2021,** *16* (3), 1376-1418.
17. Shamir, M.; Bar-On, Y.; Phillips, R.; Milo, R., SnapShot: Timescales in Cell Biology. *Cell* **2016,** *164* (6), 1302-1302.e1.
18. Rappez, L.; Stadler, M.; Triana, S.; Gathungu, R. M.; Ovchinnikova, K.; Phapale, P.; Heikenwalder, M.; Alexandrov, T., SpaceM reveals metabolic states of single cells. *Nature Methods* **2021,** *18* (7), 799-805.
19. Nemes, P.; Vertes, A., Laser Ablation Electrospray Ionization for Atmospheric Pressure, in Vivo, and Imaging Mass Spectrometry. *Analytical Chemistry* **2007,** *79* (21), 8098-8106.
20. Takáts, Z.; Wiseman, J. M.; Gologan, B.; Cooks, R. G., Mass Spectrometry Sampling Under Ambient Conditions with Desorption Electrospray Ionization. *Science* **2004,** *306* (5695), 471-473.
21. Cohen, L. H.; Gusev, A. I., Small molecule analysis by MALDI mass spectrometry. *Analytical and Bioanalytical Chemistry* **2002,** *373* (7), 571-586.
22. Feider, C. L.; Krieger, A.; DeHoog, R. J.; Eberlin, L. S., Ambient Ionization Mass Spectrometry: Recent Developments and Applications. *Analytical Chemistry* **2019,** *91* (7), 4266-4290.
23. Zhang, L.; Vertes, A., Single-Cell Mass Spectrometry Approaches to Explore Cellular Heterogeneity. *Angew Chem Int Ed Engl* **2018,** *57* (17), 4466-4477.
24. Duncan, K. D.; Fyrestam, J.; Lanekoff, I., Advances in mass spectrometry based single-cell metabolomics. *Analyst* **2019,** *144* (3), 782-793.
25. Hofstadler, S. A.; Severs, J. C.; Smith, R. D.; Swanek, F. D.; Ewing, A. G., Analysis of single cells with capillary electrophoresis electrospray ionization Fourier transform ion cyclotron resonance mass spectrometry. *Rapid Commun Mass Spectrom* **1996,** *10* (8), 919-22.
26. Kawai, T.; Ota, N.; Okada, K.; Imasato, A.; Owa, Y.; Morita, M.; Tada, M.; Tanaka, Y., Ultrasensitive Single Cell Metabolomics by Capillary Electrophoresis–Mass Spectrometry with a Thin-Walled Tapered Emitter and Large-Volume Dual Sample Preconcentration. *Analytical Chemistry* **2019,** *91* (16), 10564-10572.
27. Gao, J.; Yin, X.-F.; Fang, Z.-L., Integration of single cell injection, cell lysis, separation and detection of intracellular constituents on a microfluidic chip. *Lab on a Chip* **2004,** *4* (1), 47-52.
28. Filla, L. A.; Sanders, K. L.; Filla, R. T.; Edwards, J. L., Automated sample preparation in a microfluidic culture device for cellular metabolomics. *Analyst* **2016,** *141* (12), 3858-3865.
29. Li, X.; Zhao, S.; Hu, H.; Liu, Y. M., A microchip electrophoresis-mass spectrometric platform with double cell lysis nano-electrodes for automated single cell analysis. *J Chromatogr A* **2016,** *1451*, 156-163.
30. Berman, E. S. F.; Fortson, S. L.; Checchi, K. D.; Wu, L.; Felton, J. S.; Wu, K. J. J.; Kulp, K. S., Preparation of Single Cells for Imaging/Profiling Mass Spectrometry. *Journal of the American Society for Mass Spectrometry* **2008,** *19* (8), 1230-1236.
31. Sterling, H. J.; Batchelor, J. D.; Wemmer, D. E.; Williams, E. R., Effects of Buffer Loading for Electrospray Ionization Mass Spectrometry of a Noncovalent Protein Complex that Requires High Concentrations of Essential Salts. *Journal of the American Society for Mass Spectrometry* **2010,** *21* (6), 1045-1049.
32. Shehadul Islam, M.; Aryasomayajula, A.; Selvaganapathy, P. R., A Review on Macroscale and Microscale Cell Lysis Methods. *Micromachines* **2017,** *8* (3), 83.
33. Geng, T.; Lu, C., Microfluidic electroporation for cellular analysis and delivery. *Lab on a Chip* **2013,** *13* (19), 3803-3821.
34. Grigorov, É.; Kirov, B.; Marinov, M.; Galabov, V., Review of Microfluidic Methods for Cellular Lysis. *Micromachines* **2021,** *12*.

35. Krumpochova, P.; Bruyneel, B.; Molenaar, D.; Koukou, A.; Wuhrer, M.; Niessen, W. M. A.; Giera, M., Amino acid analysis using chromatography–mass spectrometry: An inter platform comparison study. *Journal of Pharmaceutical and Biomedical Analysis* **2015,** *114*, 398-407.
36. Aliu, E.; Kanungo, S.; Arnold, G. L., Amino acid disorders. *Ann Transl Med* **2018,** *6* (24), 471-471.
37. Socha, E.; Koba, M.; Kośliński, P., Amino acid profiling as a method of discovering biomarkers for diagnosis of neurodegenerative diseases. *Amino Acids* **2019,** *51* (3), 367-371.
38. Doron, G.; Klontzas, M. E.; Mantalaris, A.; Guldberg, R. E.; Temenoff, J. S., Multiomics characterization of mesenchymal stromal cells cultured in monolayer and as aggregates. *Biotechnology and Bioengineering* **2020,** *117* (6), 1761-1778.
39. Jayaraman, A.; Kumar, P.; Marin, S.; de Atauri, P.; Mateo, F.; M. Thomson, T.; J. Centelles, J.; F. Graham, S.; Cascante, M., Untargeted metabolomics reveals distinct metabolic reprogramming in endothelial cells co-cultured with CSC and non-CSC prostate cancer cell subpopulations. *PLOS ONE* **2018,** *13* (2), e0192175.
40. Krick, T.; Verstraete, N.; Alonso, L. G.; Shub, D. A.; Ferreiro, D. U.; Shub, M.; Sánchez, I. E., Amino Acid metabolism conflicts with protein diversity. *Mol Biol Evol* **2014,** *31* (11), 2905-2912.
41. Chilmonczyk, M. A.; Kottke, P. A.; Stevens, H. Y.; Guldberg, R. E.; Fedorov, A. G., Dynamic Mass Spectrometry Probe (DMSP) for ESI-MS Monitoring of Bioreactors for Therapeutic Cell Manufacturing. *Biotechnology and Bioengineering* **2018,** *0* (ja).
42. Arscott, S., SU-8 as a material for lab-on-a-chip-based mass spectrometry. *Lab on a Chip* **2014,** *14* (19), 3668-3689.
43. Regehr, K. J.; Domenech, M.; Koepsel, J. T.; Carver, K. C.; Ellison-Zelski, S. J.; Murphy, W. L.; Schuler, L. A.; Alarid, E. T.; Beebe, D. J., Biological implications of polydimethylsiloxane-based microfluidic cell culture. *Lab on a Chip* **2009,** *9* (15), 2132-2139.
44. Toepke, M. W.; Beebe, D. J., PDMS absorption of small molecules and consequences in microfluidic applications. *Lab Chip* **2006,** *6* (12), 1484-6.
45. Mukhopadhyay, R., When PDMS isn't the best. *Analytical Chemistry* **2007,** *79* (9), 3248-3253.
46. Kranjc, M.; Miklavčič, D., Electric Field Distribution and Electroporation Threshold. In *Handbook of Electroporation*, Miklavčič, D., Ed. Springer International Publishing: Cham, 2017; pp 1043-1058.
47. Morshed, B. I.; Shams, M.; Mussivand, T., Electrical Lysis: Dynamics Revisited and Advances in On-chip Operation. *Critical Reviews in Biomedical Engineering* **2013,** *41* (1), 37-50.